CHEMISTRY
A European Journal

A Journal of
ChemPubSoc Europe

Accepted Article

Title: Palladium-catalyzed cross-coupling reactions controlled by non-covalent Zn…N interactions

Authors: Rafael Gramage-Doria, Mohamed Kadri, Jingran Hou, Vincent Dorcet, Thierry Roisnel, Lazhar Bechki, Abdellah Miloudi, and Christian Bruneau

This manuscript has been accepted after peer review and appears as an Accepted Article online prior to editing, proofing, and formal publication of the final Version of Record (VoR). This work is currently citable by using the Digital Object Identifier (DOI) given below. The VoR will be published online in Early View as soon as possible and may be different to this Accepted Article as a result of editing. Readers should obtain the VoR from the journal website shown below when it is published to ensure accuracy of information. The authors are responsible for the content of this Accepted Article.

To be cited as: *Chem. Eur. J.* 10.1002/chem.201604780

Link to VoR: http://dx.doi.org/10.1002/chem.201604780

Supported by
ACES

WILEY-VCH

10.1002/chem.201604780

WILEY-VCH

Palladium-catalyzed cross-coupling reactions controlled by non-covalent Zn···N interactions

Mohamed Kadri,[a,b,c] Jingran Hou,[a] Vincent Dorcet,[d] Thierry Roisnel,[d] Lazhar Bechki,[b] Abdellah Miloudi,[c] Christian Bruneau,[a] and Rafael Gramage-Doria*[a]

Abstract: Non-covalent interactions between halopyridine substrates and catalytically inert building blocks, namely zinc(II)-porphyrins and zinc(II)-salphens, influence the catalytic outcome of Suzuki-Miyaura and Mizoroki-Heck palladium-catalyzed cross-coupling reactions. The weak Zn···N interactions between halopyridine substrates and zinc(II)-containing porphyrins and salphens respectively, were studied by a combination of ^{1}H NMR spectroscopy, UV-vis studies, Job-Plot analysis and, in some cases, X-ray diffraction studies. Additionally, the former studies revealed unique supramolecular polymeric and dimeric rearrangements in the solid state featuring weak Br···N (halogen bonding), C-H···π, Br···π and π···π interactions. The reactivity of halopyridine substrates in homogeneous palladium-catalyzed cross-coupling reactions was found to correlate with the binding strength between the zinc(II)-containing scaffolds and the corresponding halopyridine. Such observation is explained by the unfavourable formation of inactive over-coordinated halopyridine···palladium species. The presented approach is particularly appealing for those cases where substrates and/or products deactivate (or partially poison) a transition metal catalyst.

[a] M. Kadri, J. Hou, Dr. C. Bruneau, Dr. R. Gramage-Doria
Organometallics: Materials and Catalysis Laboratory
Institut des Sciences Chimiques de Rennes - UMR 6226
CNRS - Université de Rennes 1
35042 Rennes Cedex (France)
E-mail: rafael.gramage-doria@univ-rennes1.fr
[b] M. Kadri, Dr. L. Bechki
Département de Chimie
Université Kasdi Merbah d'Ouargla
30000 Ouargla (Algeria)
[c] M. Kadri, Prof. A. Miloudi
Ecole Nationale Polytechnique d'Oran
Laboratoire de Chimie Fine, Université d'Oran-1 Ahmed Ben Bella
31100 Oran (Algeria)
[d] V. Dorcet, Dr. T. Roisnel
X-ray Diffraction Centre
Institut des Sciences Chimiques de Rennes - UMR 6226
CNRS - Université de Rennes 1
35042 Rennes Cedex (France)

Supporting information for this article is available on the WWW under http://dx.doi.org/XXX.

Introduction

Developments on homogeneous catalysis are paving the track towards a more environmental-friendly and sustainable society.[1] In this context, transition metal catalysis plays a key role in both industry and academia. It provides access to highly functionalized molecules starting from readily available substrates due to the high versatility offered by transition metal-based catalysts.[2] As such, the reactivity of a catalyst is mainly exploited by modification of the properties of the metal centre, either by ligand design[3] (including redox-active[4] and proton-responsive ligands)[5] or, more recently, by second coordination sphere effects via catalyst encapsulation[6] or substrate-catalyst interactions.[7] These approaches are extremely powerful and will undoubtedly continue to show their potential. In parallel to that, new ways to control catalytic reactions are always appealing, especially regarding extremely important issues such as those cases where substrates and/or products inhibit or significantly decrease the activity of a transition metal catalyst.[8] Indeed, this is sometimes the case for nitrogen-containing chemicals, a major class of products relevant to agrochemistry, pharmacology and materials science.[9]

Consequently, our attention was drawn to pyridyl-containing substrates since it is known that their nitrogen lone pair may interact with the metal catalyst leading to deactivation pathways (Scheme 1).[10] For instance, regarding the behaviour of halopyridine derivatives as substrates in palladium-catalyzed cross-coupling reactions,[11] the catalytically relevant palladium centre can compete between (1) species belonging to the catalytic cycle (Scheme 1, left) and (2) nitrogen lone pair over-coordination, which inhibits the catalytic event or significantly decreases the reactivity of the catalyst (Scheme 1, right).[12] A classic approach relies on the covalent modification of pyridines into pyridinium salts or pyridine *N*-oxides before carrying out the transition metal-catalyzed transformation. These approaches have been elegantly demonstrated in the case of iridium-catalyzed hydrogenation reactions,[13] copper-catalyzed oxidations[10] and C-H bond functionalization reactions.[14]

This article is protected by copyright. All rights reserved.

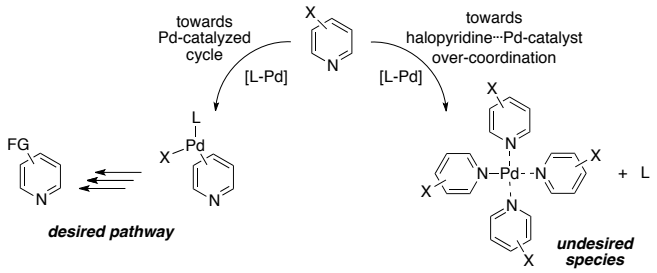

Scheme 1. General overview showing the two different possible pathways (left and right) occurring in palladium-catalyzed reactions employing halopyridines as substrates. X = halide, L = ligand, FG = functional group.

Besides catalyst fine-tuning, one may wonder whether covalent modification of the substrate is the only option to prevent undesired pyridine···catalyst over-coordination or if weak, non-covalent interactions would also have a positive effect on the outcome of catalytic reactions. With this in mind, we envisioned that the reactivity of halopyridine derivatives might be affected, at some extent, by the presence of additional building blocks able to non-covalently interact with their nitrogen lone pair if the following two considerations simultaneously operate: (1) the nitrogen lone pair from the halopyridine derivative should exclusively bind to the catalytically inert building block; and (2) the catalytically-relevant metal centre will have to exclusively coordinate to the ligand, likely a phosphane ligand in the case of palladium-catalyzed cross-coupling reactions (Scheme 2).

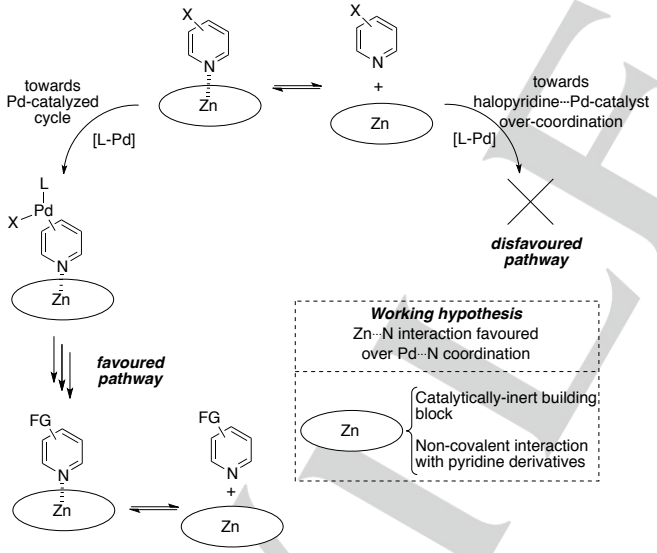

Scheme 2. Working hypothesis in order to prevent undesired halopyridine…palladium-catalyst over-coordinated species exploiting a supramolecular approach. X = halide, L = ligand, FG = functional group.

With this aim, we decided to employ zinc(II)-containing porphyrins and salphens as catalytically inert building blocks because (1) they do preferentially bind to hard pyridine motifs instead of soft phosphane ligands,[15] (2) they are chemically stable in most transition metal catalysis[16] even at high temperatures,[17] (3) the transmetallation of zinc(II) ions by other transition metals remains difficult unless extremely harsh acidic conditions or strong coordinating ligands (such as thiols) are employed,[18] or polar coordinating solvents like tetrahydrofuran or methanol are used[19] and (4) the zinc(II) centre generally adopts a well-defined, tetragonal pyramidal geometry in the presence of pyridine-containing molecules[15] in contrast to simple zinc(II)-containing salts that lead to different types of aggregated species with unpredictable stoichiometries due to the multiple coordination geometries (tetragonal, trigonal bipyridamidal, octahedral,…) the zinc(II) cation can adopt.[20] Herein, we show that (*ortho*, *meta* and *para*) bromo- and chloro-pyridine derivatives react differently in the palladium-catalyzed Suzuki-Miyaura and Mizoroki-Heck cross-coupling reactions depending on the binding strength between them and the catalytically inert zinc(II)-containing porphyrin or salphen building blocks. It will be demonstrated that the substrate reactivity can be controlled via modification of the substrate in a supramolecular manner.

Results and Discussion

Self-assembly studies

Based on previous observations which indicate that pyridine derivatives reversibly bind in a 1:1 stoichiometry to zinc(II)-porphyrins and zinc(II)-salphens with association constants ($K_{1:1}$) ranging from 10^3 to 10^6 M^{-1},[15] benchmark compounds **A** and **B** were selected as catalytically inert building blocks for this study (Figure 1, top). First, the binding capabilities of **A** and **B** towards chloro- and bromopyridine substrates **1**-**6** (Figure 3, bottom) were investigated by ^{1}H NMR spectroscopy and UV-vis titrations that enabled quantitative determination of the strength of the Zn···N interaction between the halopyridine derivatives and **A** and **B**. In some cases, the self-assembly formation between the halopyridine derivative and zinc(II)-containing building blocks **A** and **B** was corroborated by X-ray diffraction studies and their solid state features will be discussed below.

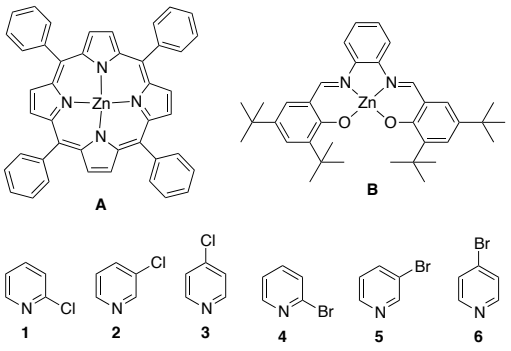

Figure 1. Catalytically inert building blocks **A** and **B** employed in this study (top) and halopyridine derivatives **1**-**6** used as substrates in this study (bottom).

This article is protected by copyright. All rights reserved.

According to ^{1}H NMR spectroscopy studies, zinc(II)-porphyrin **A** reversibly interacts with *meta*- and *para*-substituted halopyridines **2**, **3**, **5** and **6** considering the important up-field shifts observed for the proton signals belonging to the pyridine moieties upon equimolar combination of halopyridines and **A** (Table 1). For example, the *ortho*-protons belonging to **2**, **3**, **5** and **6** are up-field shifted between *ca.* 3-5 ppm upon interaction with **A** (Table 1, entries 2, 3, 5 and 6). On the other hand, *ortho*-substituted halopyridines **1** and **4** do not interact at all with **A** since the chemical shifts of the protons belonging to **1** and **4** remained unchanged in the presence of **A** (Table 1, entries 1 and 4). Such observation is further evidenced by UV-vis titrations since addition of aliquots of **1** (and **4**) to a solution of **A** does not modify the UV-vis spectrum (see the Supporting Information). The lack of interaction between bulky *ortho*-substituted pyridines and zinc(II)-porphyrins has already been reported and attributed to important steric effects.[21] The association constants ($K_{1.1}$) of **A** with *meta*- and *para*-substituted **2**, **3**, **5** and **6** halopyridine derivatives determined by UV-vis titrations using toluene as solvent were found to be 1.0 x 10^4, 9.0 x 10^3, 1.9 x 10^4 and 1.9 x 10^4 M^{-1}, respectively (see the Supporting Information).[22] Although UV-vis changes during titration were small, they were sufficient to produce well-behaved titration curves, which were used to calculate the association constants $K_{1.1}$ (see the Supporting Information).[22d,e] The binding constants $K_{1.1}$ determined for **2•A** and **5•A** are only slightly higher compared to previous reports in which the titrations were performed using a different solvent; i.e. dichloromethane.[23] In the case of **6•A**, the binding constant compares well with the one observed between **6** and a zinc(II)-porphyrin similar to **A**.[24] In all four cases (**2•A**, **3•A**, **5•A** and **6•A**), Job-Plot analysis indicated the formation of discrete 1:1 self-assembly species between **A** and **2**, **3**, **5** and **6**, respectively (see the Supporting Information).[22]

Table 1. ^{1}H NMR chemical shift variations ($\Delta\delta$) resulting from the equimolar combination of **1**-**6** with **A** and **B**, respectively,[a] and corresponding binding constants ($K_{1.1}$).[b]

Entry	Supramolecular substrate	$\Delta\delta_{o\text{-}H}$ (ppm)	$\Delta\delta_{o\text{-}H}$ (ppm)	$\Delta\delta_{m\text{-}H}$ (ppm)	$\Delta\delta_{m\text{-}H}$ (ppm)	$\Delta\delta_{p\text{-}H}$ (ppm)	$K_{1.1}$ (M^{-1})
1	**1•A**	0	n.a.	0	0	0	<1
2	**2•A**	3.9	3.8	1.5	n.a.	0.4	1.0 x 10^4
3	**3•A**	2.9	n.a.	0.8	n.a.	n.a.	9.0 x 10^3
4	**4•A**	0	n.a.	0	0	0	<1
5	**5•A**	4.1	3.9	1.8	n.a.	0.2	1.9 x 10^4
6	**6•A**	4.7	n.a.	1.5	n.a.	n.a.	1.9 x 10^4
7	**1•B**	0.1	n.a.	0.1	0.1	<0.1	2.5 x 10^3
8	**2•B**	<0.1	0.1	0.2	n.a.	0.2	6.2 x 10^5
9	**3•B**	0.1	n.a.	0.4	n.a.	n.a.	2.9 x 10^6
10	**4•B**	0.1	n.a.	0.1	<0.1	<0.1	5.2 x 10^3
11	**5•B**	<0.1	0.1	0.3	n.a.	0.3	3.7 x 10^6
12	**6•B**	0.1	n.a.	0.3	n.a.	n.a.	2.9 x 10^6

[a] Chemical shifts variation observed for the halopyridine protons. ^{1}H NMR spectroscopy performed at room temperature employing $CDCl_3$ as solvent for the case of **A** (entries 1-6) and toluene-d_8 for the case of **B** (entries 7-12). n.a. = not applied. [b] Determined by UV-vis titrations (toluene as solvent), errors estimated to be < 15%.

The self-assembly formation of **2•A**, **5•A** and **6•A** was further confirmed by X-ray diffraction studies performed on single crystals (Figure 2). A 1:1 stoichiometry between the corresponding halopyridine and zinc(II)-porphyrin **A** was evidenced. The three X-ray molecular structures indicated a clear pyridine···zinc(II)-porphyrin interaction considering the very short Zn···N distances observed ($d_{Zn...N}$ = 2.195 Å in **2•A**, $d_{Zn...N}$ = 2.182 Å in **5•A**, and $d_{Zn...N}$ = 2.164 Å in **6•A**, Figure 2). Interestingly, **6•A** gave rise to a unidirectional supramolecular polymer in the solid state stabilized by halogen bonding with weak Br···N interactions between the bromine atom from **6** and a

Accepted Manuscript

This article is protected by copyright. All rights reserved.

nitrogen atom belonging to the central core of a neighbouring molecule **A** ($d_{Br\cdots N}$ = 2.981 Å, Figure 3).[25]

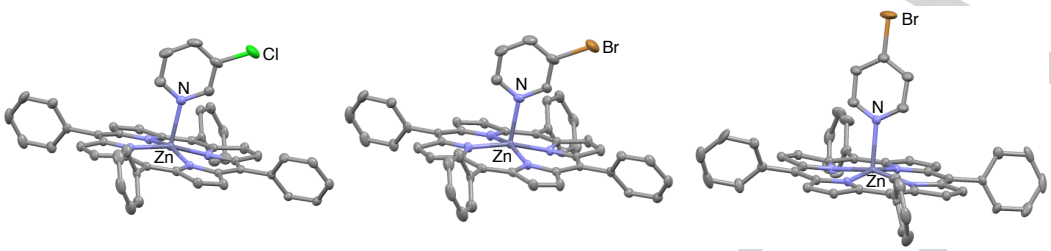

Figure 2. ORTEP drawing of **2•A** (left), **5•A** (middle) and **6•A** (right) with thermal ellipsoids at 50% probability. All hydrogen atoms and solvent molecules are omitted for clarity.

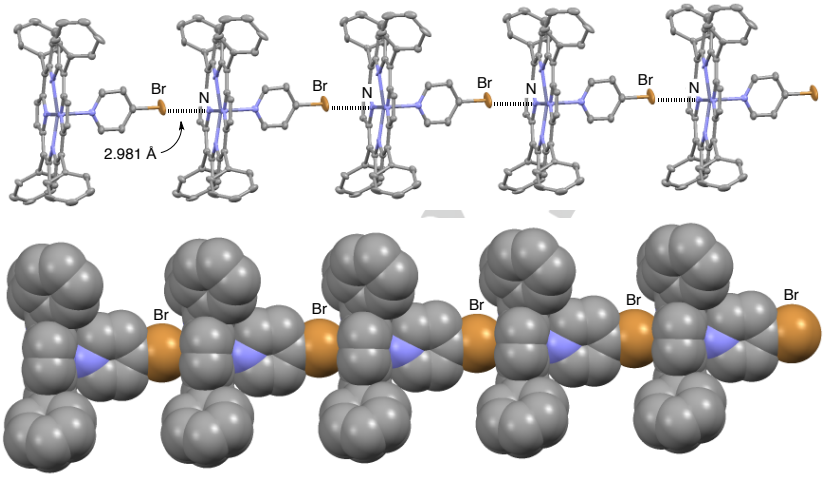

Figure 3. Supramolecular polymeric structure of **6•A** displayed as ORTEP drawing with thermal ellipsoids at 50% probability indicating weak Br···N interactions (top) and as space-fill representation (bottom). All hydrogen atoms are omitted for clarity.

The ability of building block **B** to interact with halopyridine substrates **1**-**6** was also investigated. ^{1}H NMR spectroscopy analysis of stoichiometric combination of **B** with **1**-**6** indicated that all halopyridine derivatives did interact with **B** as inferred from the observed chemical shift variations (Table 1, entries 7-12). Contrary to the behavior of **A** towards *ortho*-substituted pyridines **1** and **4** (Table 1, entries 1 and 4), the zinc(II)-salphen building block **B** also interacted with **1** and **4** (Table 1, entries 7 and 10). However, qualitatively, **B** was more strongly bound to *meta*- and *para*-substitituted halopyridines than to *ortho* ones since the chemical shifts variations were more significant for the formers with $\Delta\delta$ up to 0.4 ppm, which further was supported by the binding constants values. Indeed, the binding constants $K_{1:1}$ determined by UV-vis titrations lied in the range 10^5-10^6 M^{-1} for the *meta*- and *para*-substituted halopyridines **2**, **3**, **5** and **6** (Table 1, entries 8, 9, 11 and 12; see the Supporting Information), whereas *ortho*-substituted halopyridines **1** and **4** provided lower values around 10^3 M^{-1} (Table 1, entries 7 and 10; see the Supporting Information). Job-Plot analyses also indicated the formation of 1:1 assemblies between **B** and substrates **1**-**6** (see the Supporting Information). Interestingly, **A** and **B** have different coordinative trends towards the different halopyridine derivatives, which make them suitable candidates for the further evaluation in homogeneous transition metal catalysis (*vide infra*). It must be noted that the different supramolecular behaviours between zinc(II)-salphens and zinc(II)-porphyrins towards *ortho*-substituted pyridines were not unprecedented.[26]

In addition, the self-assembly formation of **2•B**, **4•B** and **5•B** was unambiguously determined by X-ray diffraction studies performed on single crystals (Figure 4). The molecular structures indicated the binding of the corresponding halopyridine derivative to the zinc(II) centre of salphen **B** with Zn···N distances as short as 2.150 Å for **2•B**, 2.170 Å for **4•B** and 2.144 Å for **5•B** (Figure 4). The larger Zn···N distance observed in **4•B** compared to **5•B** and **2•B** likely originated from the steric repulsion generated by the *ortho*-located bromine atom around the zinc(II)-salphen platform **B**, which slightly tilts the pyridine ring forcing a non-optimal Zn···N interaction.[27] The Zn···N distances observed in **2•B**, **4•B** and **5•B** (Figure 4) are shorter than those observed for zinc(II)-porphyrin-containing **2•A**, **5•A** and **6•A** (Figure 2). This finding correlates well with the different

Accepted Manuscript

This article is protected by copyright. All rights reserved.

coordination strength established by UV-vis titrations (Table 1). As a consequence, in each series, a higher association constant ($K_{1.1}$) corresponds with a shortening of the Zn···N distance.

It is interesting to point out that the halide atoms in **2•B**, **4•B** and **5•B** are pointing towards a different direction in the solid state (Figure 4). For example, in the case of **2•B**, the chlorine atom points towards one phenolic ring, thus forcing a slight bend coordination of the halopyridine towards the zinc(II)-salphen core (Figure 5). The origin (or consequence) of such behaviour results in supramolecular C-H···π interactions between the pyridinic *para*-protons (*p*-H) and the phenylene ring of an opposed salphen scaffold (Figure 5, left and middle).[28] The distances observed between the *p*-H atom and five carbon atoms (C_1-C_5) from the phenylene ring are 2.821 Å, 2.766 Å, 2.780 Å, 2.825 Å and 2.894 Å, respectively (Figure 5, right).

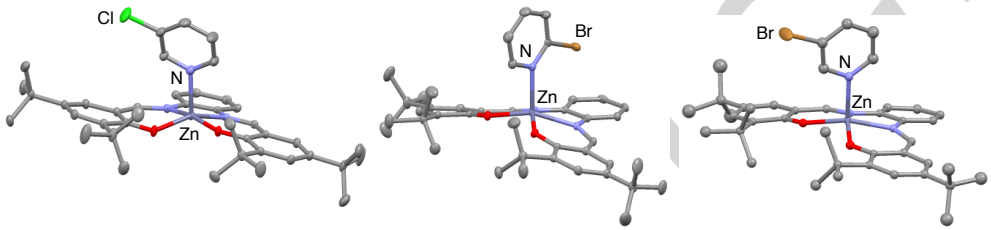

Figure 4. ORTEP drawing of **2•B** (left), **4•B** (middle) and **5•B** (right) with thermal ellipsoids at 50% probability. All hydrogen atoms are omitted for clarity.

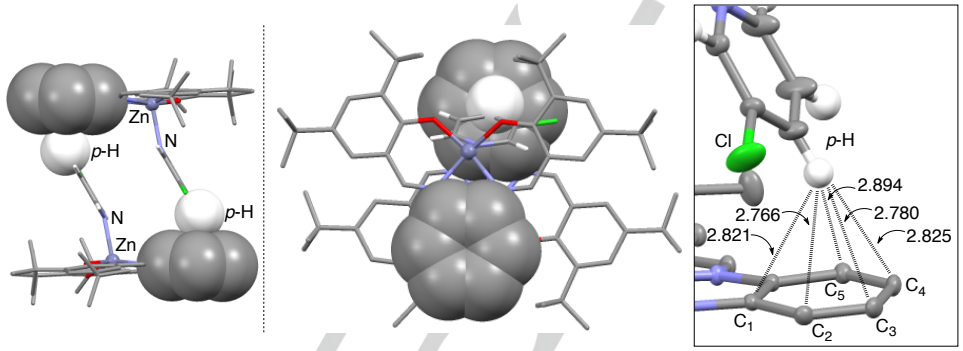

Figure 5. Supramolecular dimeric structure of **2•B** displayed as capped stick representation (space fill representation for key hydrogen and benzene ring) highlighting weak C-H···π interactions from side view (left) and bottom-up view (middle); and zoom of the supramolecular dimeric structure of **2•B** displayed as ORTEP drawing with thermal ellipsoids at 50% probability highlighting the key *p*-H···C distances responsible for weak C-H···π interactions (right). Non-relevant hydrogen atoms are omitted for clarity.

On the other hand, in the solids state, the bromine atom of **4•B** is oriented towards the phenylene ring backbone whereas the bromine atom in **5•B** is oriented towards the *tert*-butyl groups of **B** in order to minimize steric repulsions. This subtle steric effect between *ortho*- and *meta*-bromopyridine **4** and **5** is likely at the origin of a different supramolecular rearrangement in the solid state of **4•B** and **5•B** respectively. For instance, **4•B** gives rise to a *zig-zag* supramolecular polymer in the solid state with short Br···π interactions (Figure 6).[29] The bromine atom interacts with the aryl ring of the phenylene unit belonging to the zinc(II)-salphen molecule which is binding to ($d_{Br...C1}$ = 3.280 Å, Figure 6) as well as with the phenylene unit belonging to a neighbouring zinc(II)-salphen molecule ($d_{Br...C2}$ = 3.441 Å and $d_{Br...C3}$ = 3.536 Å, Figure 6).

Accepted Manuscript

This article is protected by copyright. All rights reserved.

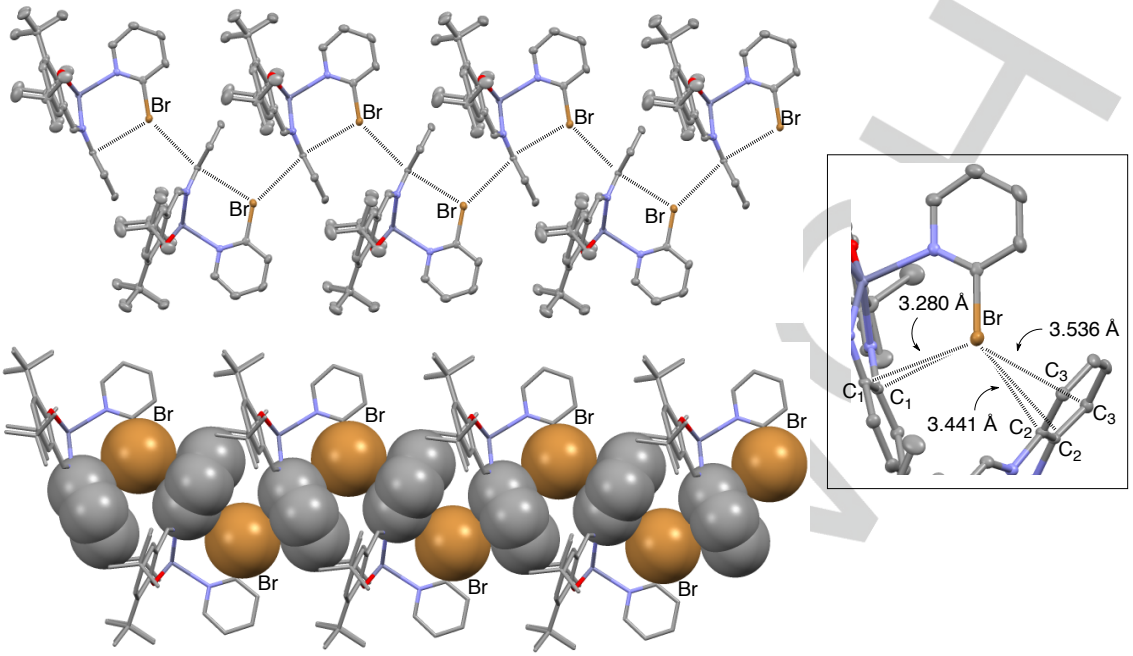

Figure 6. Supramolecular polymeric structure of **4•B** displayed as ORTEP drawing with thermal ellipsoids at 50% probability indicating weak Br···π interactions (top); capped stick representation with the key bromine atom and phenylene units in space-fill representation to highlight their interaction (bottom); and zoom of the supramolecular polymeric structure of **4•B** displayed as ORTEP drawing with thermal ellipsoids at 50% probability highlighting the key Br···C distances responsible for weak Br···π interactions (right). All hydrogen atoms are omitted for clarity.

Contrary to **4•B**, **5•B** prefers to adopt a supramolecular dimeric structure taking benefit from π···π interactions between two aromatic units belonging to two different molecules of **5•B** ($d_{C1...C4}$ = 3.324 Å, $d_{C2...C5}$ = 3.382 Å and $d_{C3...C5}$ = 3.301 Å, Figure 7).[30] The unexpected supramolecular arrangements observed in the solid state in **6•A**, **2•B**, **4•B** and **5•B** involving a plethora of weak Br···N, C-H···π, Br···π and π···π interactions (Figures 2-7), respectively, are however not as strong as the Zn···N interactions whose distances are much shorter (< 2.2 Å) than the above-mentioned set of weak interactions (*ca.* 2.8-3.5 Å). The Zn···N interaction must be regarded as the *strongest* interaction from the *weakest* ones described below. Nevertheless, these additional observations clearly expand the fundamental understanding of the supramolecular behaviour of zinc(II)-containing scaffolds involving weak interactions in the solid state

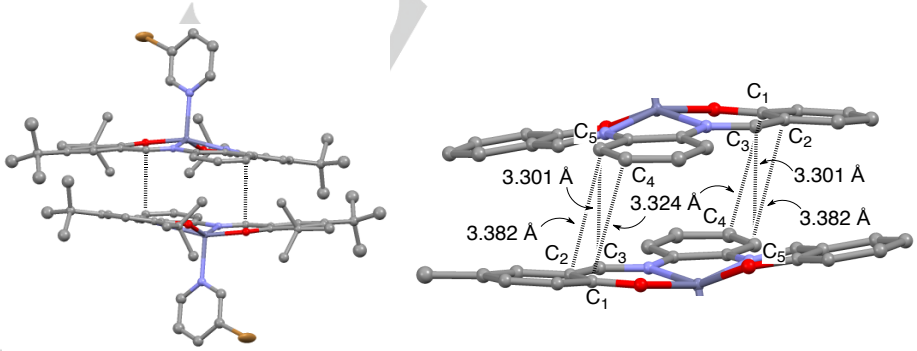

Figure 7. Supramolecular dimeric structure of **5•B** displayed as ORTEP drawing with thermal ellipsoids at 50% probability indicating π···π interactions in dashed lines (left) and zoom of the supramolecular dimeric structure of **5•B** displayed as ORTEP drawing with thermal ellipsoids at 50% probability highlighting the key C···C distances responsible for weak π···π interactions (right, *tert*-butyl groups were removed for clarity). All hydrogen atoms are omitted for clarity.

Accepted Manuscript

This article is protected by copyright. All rights reserved.

Palladium-catalyzed experiments

After studying the different binding properties of **A** and **B** (*vide supra*) towards different halopyridine derivatives suitable to undergo palladium-catalyzed cross-coupling reactions, we first studied in detail the reactivity of 2-bromopyridine (**4**) and 3-bromopyridine (**5**) in the presence of one equivalent of **A** under standard Suzuki-Miyaura cross-coupling reaction conditions (1 mol% of $Pd(OAc)_2$, 2 mol% of PPh_3, 2 equivalents of K_2CO_3 and 2 equivalents of $PhB(OH)_2$).[31] Since **A** does not bind to **4** (Table 1, entry 4), a similar catalytic outcome independently whether **A** is present or not in the reaction mixture was expected. On the contrary, since **A** does bind to **5**, different catalytic behaviours when performing the catalysis with or without zinc(II)-porphyrin **A** was anticipated. Indeed, the kinetic profile of **4** did not significantly change as compared to the reaction carried out in the presence of one equivalent of building block **A** (Figure 8, top). On the contrary, when the same catalytic experiments were carried out with 3-bromopyridine **5**, a different kinetic profile was observed in the presence of **A** (Figure 8, bottom). For instance, in the presence of **A**, full conversion of **5** was reached in four hours; whereas in the absence of **A**, full conversion was attained only after ten hours (Figure 8, bottom). At the end of the corresponding catalytic reactions, an acidic work-up was performed to check by ^{1}H NMR spectroscopy that the molecular structure of **A** remained intact under the catalytic reaction conditions (see Experimental Section). It is important to note that the zinc(II)-porphyrin **A** was not involved in transmetallation reaction with palladium and did not react with any other reagents under the reaction conditions. The use of catalytic amounts of **A** did not give satisfactory results; and the utilization of more than one equivalent of **A** did not alter the kinetic effect observed when using one equivalent of **A**. These findings indicated that to observe the positive kinetic effect (Figure 8, bottom), at least one equivalent of **A** is required in the reaction mixture to ensure full halopyridine···zinc(II)-porphyrin interaction for the studied palladium-catalyzed Suzuki cross-coupling reaction. Interestingly, the nature of the solvent also had a strong influence on this effect. For instance, replacing toluene (which is a well-known solvent to maximize pyridine···zinc(II)-porphyrin interactions)[32] for *N*,*N*-dimethylformamide (DMF) gave rise to very similar results in the conversion of **5** with and without **A** (see the Supporting Information). As it could be expected, with strongly coordinating solvents such as DMF, the halopyridine···zinc(II)-porphyrin interaction is negligible, and thus, the reactivities observed with **5** remained similar (85% conversion after 2 hours with or without **A** in the reaction mixture, see the Supporting Information). In addition, the kinetic behaviour of the reactions with 2-chloropyridine (**1**) and 3-chloropyridine (**2**) as substrates in the presence of **A** compares well with their bromo-analogues **4** and **5**, although they required longer reaction time to reach completion (see Figure S7 in the Supporting Information).

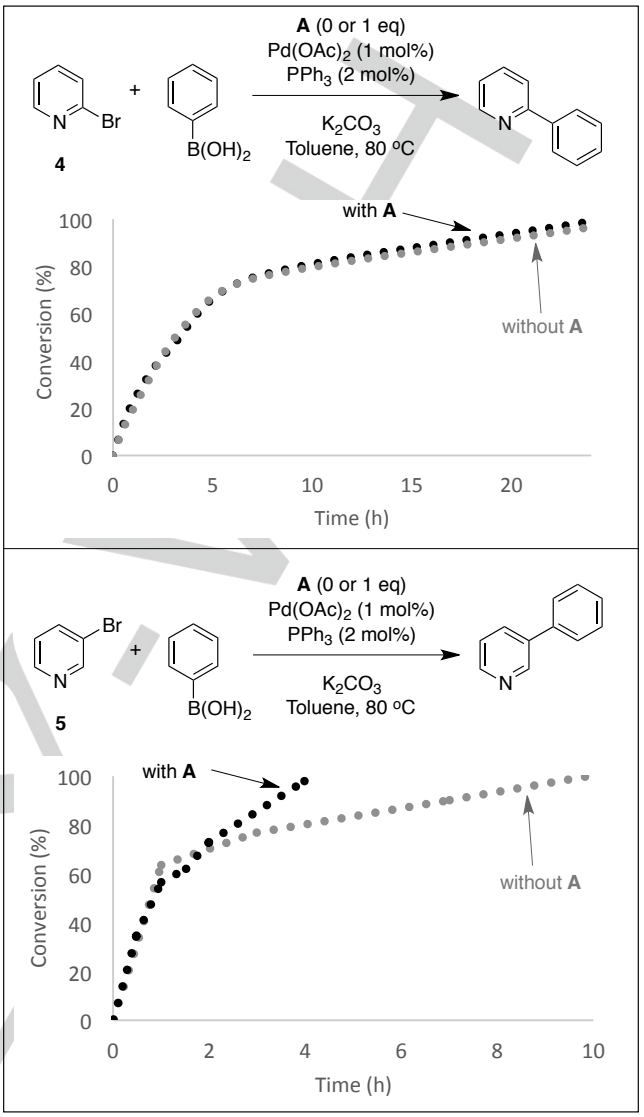

Figure 8. Top: Plot of conversion of **4** versus time under Suzuki-Miyaura conditions with the presence of **A** (black points) and without the presence of **A** (grey points). Bottom: Plot of conversion of **5** versus time under Suzuki-Miyaura conditions with the presence of **A** (black points) and without the presence of **A** (grey points).

To get a better understanding on the origin of the kinetic behaviour observed in the conversion of **5** caused by the presence of **A**, the potential energy surfaces (PM3 calculations) of **5** and the supramolecular substrate **5•A** were qualitatively evaluated (Figure 9). The bromine atom has a slightly higher Lewis acid character (blue) in **5•A** than in **5** (Figure 9). Although one could imagine that the binding of zinc(II)-porphyrin **A** to **5** would increase the reactivity of the C–Br bond towards the palladium-promoted oxidative addition step, such a statement was not likely since almost identical initial activities were observed for the reaction occurring with or without **A** (Figure 8, bottom) unless the oxidative addition of C–Br to the Pd^0 centre is not the determining step of the catalytic cycle. Additionally, the

Accepted Manuscript

This article is protected by copyright. All rights reserved.

ability of **A** and **5** to interact each other in the presence of the palladium catalyst under the reaction conditions, namely 1 mol% of $Pd(OAc)_2$ and 2 mol% of triphenylphosphine (PPh_3), was investigated by ^1H NMR spectroscopy (see the Supporting Information). Similar chemical shift variations were observed for the pyridinic protons as it was the case in Table 1, entry 5. In addition, the $^{31}P\{^1H\}$ NMR spectrum showed the appearance of a new peak at *ca.* 25 ppm belonging to phosphane-coordinated palladium species,[33] indicating that the formation of palladium-triphenylphosphine species was compatible with the supramolecular self-assembly substrate **5•A**. As such, the presence of the palladium-triphenylphosphine catalyst did not inhibit the self-assembly formation of the supramolecular substrate **5•A**. The catalytically inert platform **A** trapped the halopyridine substrate **5** avoiding the formation of halopyridine···palladium species, thus it indirectly favoured the formation of active palladium-triphenylphosphine catalytic species. It is relevant to mention that we also found by that the other reagents used in the catalytic experiments (potassium carbonate and phenylboronic acid) did not alter the self-assembly formation of **5•A**.

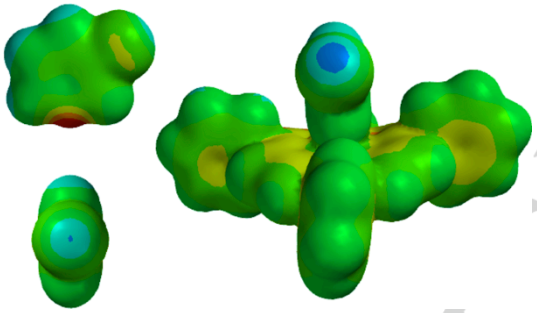

Figure 9. Potential energy surfaces calculated with PM3 showing a very small increase of Lewis acidity (blue) of the bromine atom in **5•A** (right) compared to **5** (front view and side view, left).

Having established the unique ability of zinc(II)-porphyrin **A** to modify the reactivity of bromopyridine **5** in a non-covalent manner, the reactivity of the other halopyridine derivatives in the presence of one equivalent of catalytically inert building block **A** under standard palladium-catalyzed Suzuki-Miyaura cross-coupling reaction conditions was also studied. Representative results are summarized in Figure 10, in which at a given time the conversion of the halopyridine is reported with and without the presence of **A**. As it is the case for the reactivity of 2-bromopyridine **4** (Figure 8, top), 2-chloropyridine **1** reacted in the same way with and without the presence of **A** giving conversions of 55% after four hours in both cases (Figure 10) due to the lack of interaction between **1** and **A** (*vide supra*). Interestingly, *meta*- and *para*-substituted halopyridines, which are known to non-covalently interact with **A** (*vide supra*), reacted more efficiently in the presence of **A**. For example, 20% conversion of 3-chloropyridine **2** was observed in the presence of **A** after two hours (Figure 10), whereas without the presence of **A** the conversion dropped to 9% (Figure 10). In the case of 4-chloropyridine (**3**), the presence of **A** resulted in an increase of the conversion of **3** from 37 to 63% after four hours (Figure 10). Finally, 4-bromopyridine (**6**) gave an increase of its conversion around 10% (from 62 to 73% conversion) as compared to the reaction carried out without **A** (Figure 10). In summary, the catalytic outcomes observed for halopyridines **1**-**6** followed the same trend, with the conversion of *ortho*-substituted compounds (**1** and **4**) not being affected by the presence of zinc(II)-porphyrin **A**, whilst the conversions of *meta*- and *para*-substituted substrates (**2**, **3**, **5** and **6**) were higher when **A** was present in the reaction mixture.

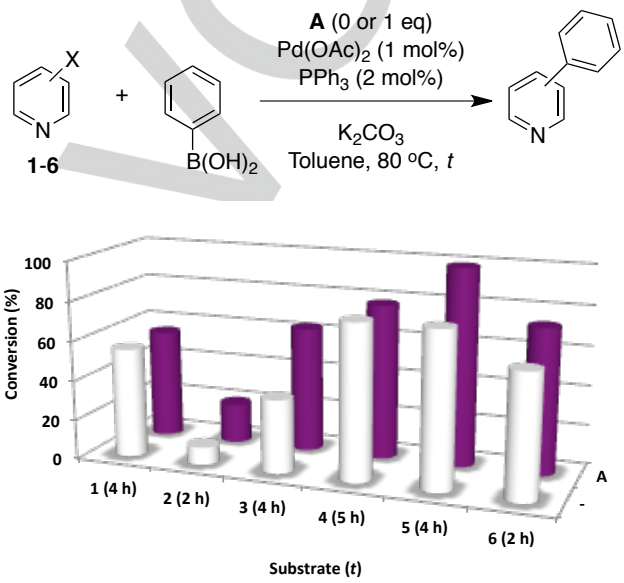

Figure 10. Influence of the presence of catalytically-inert building block **A** in the conversion of halopyridines **1**-**6** at a given time (in brackets) in Suzuki-Miyaura cross-coupling reactions. Reaction conditions: $[Pd(OAc)_2]$ (2.5×10^{-3} mmol, 1 mol%), PPh_3 (5×10^{-3} mmol, 2 mol%), halopyridine (0.25 mmol), **A** (0.170 g, 0.25 mmol) -when applied-, $PhB(OH)_2$ (0.061 g, 0.5 mmol), K_2CO_3 (0.069 g, 0.5 mmol), toluene (1.25 mL), dodecane (0.057 mL), 80 °C, argon atmosphere. The conversions were determined by GC. The calibrations were based on dodecane. Reactions were performed 2-3 times. See the Supporting Information for details.

Unfortunately, building block **B** was not applicable in the palladium-catalyzed Suzuki-Miyaura cross-coupling reaction due to its decomposition by phenylboronic acid as confirmed by ^1H NMR spectroscopy studies. It is plausible that hydroxyl groups generated at the transmetallation elementary step of the catalytic cycle of the Suzuki-Miyaura cross-coupling reaction cleaved the imine bonds of **B**.[34] Interestingly, **B** was found stable under the reaction conditions employed in palladium-catalyzed Mizoroki-Heck cross-coupling reactions.[35] Consequently, the reactivity of halopyridine substrates **1**-**6** in the presence of catalytically inert building blocks **A** and **B** was evaluated in this cross-coupling reaction. Thus, 0.5 mmol of styrene and 0.25 mmol of halopyridine were reacted at 80 °C in toluene in the presence of a stoichiometric amount of **A** or **B** and cesium carbonate as base, and a catalytic amount of $Pd(OAc)_2$

Accepted Manuscript

This article is protected by copyright. All rights reserved.

(1 mol%) and PPh_3 (2 mol%). The results are summarized in Figure 11 indicating the conversion of the halopyridine derivatives at a given time. As a general trend, the conversions of halopyridines were higher in the presence of one equivalent of zinc(II)-salphen **B** than in the presence of one equivalent of zinc(II)-porphyrin **A** or without any building block (Figure 11). Interestingly, the utilization of zinc(II)-salphen **B** affected the reactivity of 2-halopyridines; a feature which was not observed with zinc(II)-porphyrin **A** as a coordinating platform. For instance, 2-chloropyridine (**1**) and 2-bromopyridine (**4**) reacted only if **B** was present in the reaction mixture leading to 12% and 16% conversion, respectively after 3 hours (Figure 11). On the other hand, no conversion was observed for 2-chloropyridine (**1**) and 2-bromopyridine (**4**) with or without **A** after 3 hours (Figure 11). This observation might be a direct consequence of the interaction of **1** and **4**, with **B**, respectively ($K_{1:1}$ = 2.5 x 10^3 M^{-1} and 5.2 x 10^3 M^{-1}, respectively, Table 1, entries 7 and 10), which leaves the palladium/phosphane catalyst more available than in the case where **A**, which did not interact at all with **1** (or **4**), is in the reaction mixture. In the case of 3- and 4-halopyridines, the conversions increased with the binding capabilities of **A** and **B** (Figure 11). For example, no conversion of 3-bromopyridine (**5**) was observed in the blank reaction after 3 hours, whereas 21% conversion was reached when the reaction was performed with **A** and 45% conversion when employing the more pyridine-coordinating building block **B** (Figure 11). As compared to the influence of the supramolecular platform **A** in the Suzuki-Miyaura reactions, the halopyridine···zinc coordination not only improved the reactivity, but more importantly, it made possible the Mizoroki-Heck reaction, which did not occur without **A** or **B** when the pyridines **1**, **2**, **4** and **5** were used (Figure 11). The overall catalytic results indicate the beneficial role of the non-covalent Zn···N interaction for those cases where substrates and/or products inhibit (or significantly decrease) the efficiency of the catalyst.

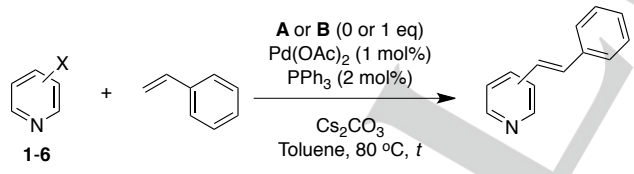

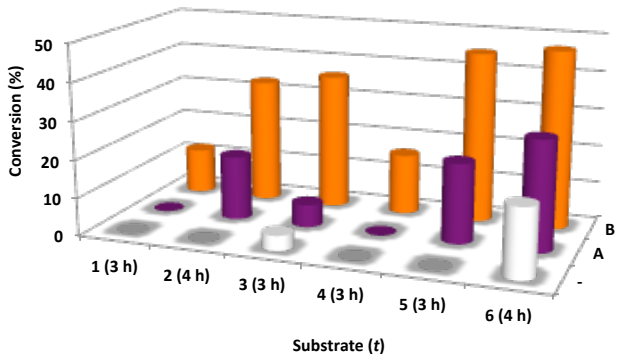

Figure 11. Influence of the presence of catalytically-inert building blocks **A** and **B** in the conversion of halopyridines **1**-**6** at a given time (in brackets) in Mizoroki-Heck cross-coupling reactions. Reaction conditions: [$Pd(OAc)_2$] (2.5 x 10^{-3} mmol, 1 mol%), PPh_3 (5x10^{-3} mmol, 2 mol%), halopyridine (0.25 mmol), **A** (0.170 g, 0.25 mmol) -when applied-, **B** (0.151 g, 0.25 mmol) -when applied-, styrene (0.052 g, 0.5 mmol), anhydrous Cs_2CO_3 (0.163 g, 0.5 mmol), toluene (1.25 mL), dodecane (0.057 mL), 80 °C, argon atmosphere. The conversions were determined by GC. The calibrations were based on dodecane. Reactions were performed 2-3 times. See the Supporting Information for details.

Robustness of A in Ru-catalyzed C-H bond functionalization

Finally, we decided to further investigate the stability of zinc(II)-containing scaffolds in other important carbon-carbon bond forming reactions, namely ruthenium(II)-catalyzed C-H bond functionalization reactions.[36] We selected typical reaction conditions[37] to perform such a transformation since the 2-phenylpyridine substrate is too bulky to interact with **A**. The same catalytic outcome (> 99% yield of the bis-arylated product) was observed regardless the presence of zinc(II)-tetraphenylporphyrin **A** in the reaction mixture (Scheme 3). As it was the case with the palladium-catalyzed experiments described above, **A** was recovered once the reaction was completed and no zinc/ruthenium transmetallation was detected. These last experiments, together with the palladium-catalyzed ones, indicated the unique robustness of zinc(II)-tetraphenylporphyrin **A** in these cross-coupling transformations.[16]

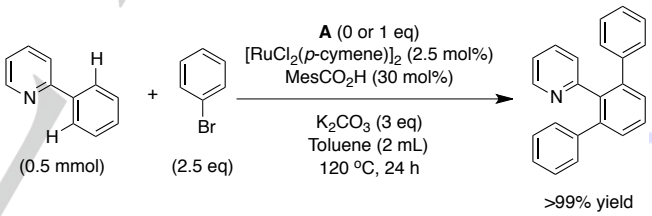

Scheme 3. Ruthenium(II)-catalyzed C-H bond functionalization of 2-phenylpyridine substrate in the presence (or not) of zinc(II)-porphyrin **A**.

Conclusions

In summary, we have introduced a new approach to control palladium-catalyzed cross-coupling reactions by modifying the properties of the pyridine substrates in a supramolecular manner without changing the properties of the palladium-phosphane catalyst. Taking benefit from non-covalent Zn···N interactions between catalytically inert building blocks and halopyridine substrates, the pathways towards palladium-catalyzed cross-coupling reactions are indirectly favoured, preventing at some extent undesired halopyridine···palladium-catalyst over-coordination pathways.

The interactions between the halopyridine substrates and zinc(II)-porphyrin **A** and zinc(II)-salphen **B**, respectively, have been studied by different spectroscopic techniques including ^1H NMR spectroscopy, UV-vis spectroscopy and X-ray diffraction studies. They indicated that *ortho*-substituted halopyridines did

Accepted Manuscript

This article is protected by copyright. All rights reserved.

not interact with **A**, whereas *meta*- and *para*-substituted halopyridines did interact with **A** and **B**, the binding constants with **B** being higher than with **A**. The influence of such different binding properties of **A** and **B** towards halopyridine derivatives was evaluated in palladium-catalyzed transformations. The Suzuki-Miyaura cross-coupling reaction studies revealed that the conversions of *meta*- and *para*-halopyridines were higher in the presence of **A** as compared to those observed in the control experiments. On the other hand, since *ortho*-halopyridines did not bind to **A**, the same kinetic profile was observed as in the control experiments. In the case of palladium-catalyzed Mizoroki-Heck cross-coupling reactions, the conversions of halopyridine substrates increased with the increase of the binding constants, the highest conversions being observed when **B** was present in the reaction mixture. The presence of **A** and **B** even made possible reactions that did not operate without these supramolecular interactions. Although it is difficult to establish the degree of catalyst inhibition caused by the substrates and/or the products in our study, the role of non-covalent Zn···N interactions to (partially) avoid catalyst poisoning has been demonstrated.

Since the approach disclosed in this contribution is operationally simple, it could be applied to other types of transition metal-catalyzed reactions (such as C-H bond functionalization, Scheme 3), in which nitrogen-containing substrates or products poison or partially deactivate a transition metal catalyst. This would be an alternative to methods based on the pre-functionalization of pyridine derivatives into *N*-protected pyridines or methods devoted to fine-tune metal catalysts. The above described weak Zn···N interactions between substituted pyridines and catalytically inert zinc(II)-containing scaffolds might be evaluated in the future for allosteric regulation in transition metal-catalyzed transformations,[38] switchable catalysis[39] and/or substrate-preorganized catalysis.[7c]

Experimental Section

General methods. All commercial reagents were used as supplied from commercial sources. All syntheses were performed in Schlenk-type flasks under argon atmosphere. Solvents were purified by solvent purification system equipped with a serie of activated filter columns or dried by conventional methods and distilled immediately prior to use. All reagents were weighed and handled in air, and refilled with an inert atmosphere of argon at room temperature. **A**[40] and **B**[41] were prepared according to literature procedures and dried under high vacuum overnight prior to use. $CDCl_3$ was passed down a 5 cm-thick alumina column and stored under nitrogen over molecular sieves (4 Å). ^{1}H NMR spectra were recorded on Bruker GPX (400 MHz) spectrometer and ^{31}P NMR spectra were recorded at 162 MHz on the same spectrometer. ^{1}H NMR spectra were referenced to residual protiated solvent (δ = 7.26 ppm for $CDCl_3$, δ = 6.97 ppm for toluene-d_8) and the ^{31}P NMR data are given relative to external H_3PO_4. UV-vis absorption spectra were recorded using Specord 205 UV-vis-NIR spectrophotometer using quartz cuvettes of 1 cm pathlength. The catalytic reactions were monitored using a Shimadzu 2014 gas chromatography equipped with EquityTM-1 Fused Silica capillary column (30 m x 0.25 mm x 0.25 mm) and a FID detector (Method: Initial temp = 60 °C, Ramp = 10 °C/min to 220 °C, hold 10 min); and the conversions were determined using dodecane as internal standard. Molecular modelling calculations were performed using PM3-Spartan molecular modelling program.

Synthesis of substrates 3 and 6. The corresponding 4-halopyridine hydrochloride salts (1 equivalent) were treated with potassium carbonate (10 equivalents) in acetonitrile as solvent at room temperature during six hours. The reaction mixture was then filtered over magnesium sulfate and evaporation of the solvents at room temperature followed by overnight drying under high vacuum yielded **3** and **6**, respectively, in virtually quantitative yield. ^{1}H NMR data match those found in the literature.[42]

General procedure for UV-vis titrations. Host-guest interactions in solution were studied by UV-vis spectroscopy. Solutions of **A** (10^{-6} M), **B** (5×10^{-5} M) and of the different substrates tested **1**-**6** (10^{-4} M for titration with **A** and 5×10^{-3} M for titration with **B**) were prepared using toluene as solvent. An increasing number of substrate equivalents were added to a solution of **A** -or **B**- (2 mL in a 1 cm cuvette cell). The host concentration was kept constant. The stoichiometry of the self-assembly substrates was studied using the method of continuous variations, by adding different ratios of guest solution, in order to add an increasing number of substrate equivalents. The association constants were calculated from the changes in absorbance at the wavelengths near to λ_{max}. Nonlinear curve fitting for 1:1 binding model was found the most suitable for all cases studied in this work. Association constants $K_{1:1}$ and asymptotic changes in absorbance ΔA were set as free parameters for fitting.[43]

General procedure for palladium-catalyzed Suzuki-Miyaura cross-coupling reactions: A Schlenk tube under an argon atmosphere was filled with the corresponding halopyridine (0.25 mmol, 1 eq), phenylboronic acid (0.061 g, 0.5 mmol, 2 eq), potassium carbonate (0.069 g, 0.5 mmol, 2 eq), dodecane (0.057 mL, internal standard reference), **A** (0.170 g, 0.25 mmol, 1 eq) -if applied- and toluene (0.75 mL). After 5 min stirring at room temperature, a solution of $[Pd(OAc)_2]$ (0.56 mg, 0.0025 mmol, 1 mol%) and triphenylphosphine (1.31 mg, 0.0050 mmol, 2 mol%) in toluene (0.5 mL) was added. The reaction mixture was placed in a preheated oil bath at 80 °C and aliquots were taken under smooth argon flow to be analyzed by GC after filtration. Once the starting materials were consumed, the reaction mixture was diluted with dichloromethane and the products extracted with an aqueous solution of HCl 2 M (3 x 20 mL). The dichloromethane fraction was dried over $MgSO_4$ before being filtrated and evaporated to dryness; ^{1}H NMR spectroscopy provided evidence of the stability of **A**. The acidic aqueous layer was basified with NaOH pellets followed by extraction with ethyl acetate (3 x 20 mL). The organic layer was dried over $MgSO_4$ before being filtrated and evaporated to dryness. The crude reaction mixture was further purified by column chromatography with a mixture of petroleum ether and ethyl acetate. Alternatively, once the starting materials were consumed, the reaction mixture was evaporated to dryness and the crude reaction mixture was further purified by column chromatography with a mixture of petroleum ether and ethyl acetate.

General procedure for palladium-catalyzed Mizoroki-Heck cross-coupling reactions: A Schlenk tube under an argon atmosphere was filled with the corresponding halopyridine (0.25 mmol, 1 eq), styrene (0.052 g, 0.057 mL, 0.5 mmol, 2 eq), anhydrous cesium carbonate (0.069 g, 0.5 mmol, 2 eq), dodecane (0.057 mL, internal standard reference), **A** (0.170 g, 0.25 mmol, 1 eq) -if applied-, **B** (0.163 g, 0.25 mmol, 1 eq) -if applied- and toluene (0.75 mL). After 5 min stirring at room temperature, a solution of $[Pd(OAc)_2]$ (0.56 mg, 0.0025 mmol, 1 mol%) and triphenylphosphine (1.31 mg, 0.0050 mmol, 2 mol%) in toluene (0.5 mL) was added. The reaction mixture was placed in a preheated oil bath at 80 °C and aliquots were taken under smooth argon flow to be analyzed by GC after filtration. Once the starting materials were consumed, the

Accepted Manuscript

This article is protected by copyright. All rights reserved.

reaction mixture was evaporated to dryness and the crude reaction mixture was further purified by column chromatography with a mixture of petroleum ether and ethyl acetate.

General procedure for ruthenium-catalyzed C-H bond functionlization: A Schlenk tube under an argon atmosphere was filled with 2-phenylpyridine (0.5 mmol, 1 eq), bromobenzene (1.25 mmol, 2.5 eq), anhydrous potassium carbonate (1.5 mmol, 3 eq), **A** (0.5 mmol, 1 eq) -if applied-, $[RuCl_2(p\text{-cymene})]_2$ (0.0125 mmol, 2.5 mol%), 2,4,6-trimethylbenzoic acid (0.15 mmol, 30 mol%) and toluene (2 mL). The reaction mixture was placed in a preheated oil bath at 120 °C and stirred during 24 hours. Back at room temperature, water (30 mL) was added and the crude reaction mixture was extracted with ethyl acetate (3 x 20 mL). The combined organic layers were dried over $MgSO_4$, filtrated and concentrated in vacuum. The ^{1}H NMR, GC/MS and TLC analysis of the crude reaction mixture indicated the exclusive formation of the bis-arylated product which was further isolated in >95% yield by column chromatography on silica gel (petroleum ether/ethyl acetate).

Supporting Information. Further experimental details including NMR data, UV-vis titration studies (including Job-Plot analysis), crystallographic details and calibration curves are provided in the supporting information. The supplementary crystallographic data for **2•A** (CCDC-1509179), **5•A** (CCDC-1509180), **6•A** (CCDC-1509181), **2•B** (CCDC-1509182), **4•B** (CCDC-1509183) and **5•B** (CCDC-1509178) can be obtained free of charge from The Cambridge Crystallographic Data Centre (CCDC) at www.ccdc.cam.ac.uk.

Acknowledgements

C.B. and R.G.-D. acknowledge the CNRS and Université de Rennes 1 for providing financial support. The Université Kasdi Merbah (Ouargla, Algeria) is acknowledged for a visiting scholarship to M.K.

Keywords: palladium catalysis • weak interactions • pyridine • porphyrin • salphen

[1] a) R. Noyori, *Nat. Chem.* **2009**, *1*, 5-6; b) K. Sanderson, *Nature* **2011**, *469*, 18-20; c) R. A. Sheldon, *Chem. Soc. Rev.* **2012**, *41*, 1437-1451; d) G. Rothenberg, *Catalysis: Concepts and Green Applications* (Wiley-VCH, Weinheim, Germany, **2008**); e) M. Beller, *Chem. Soc. Rev.* **2011**, *40*, 4891-4892.

[2] a) J. F. Hartwig, *Organotransition Metal Chemistry: From Bonding to Catalysis*, University Science Books, Sausalito, CA, USA **2009**; b) M. Beller, C. Bolm, *Transition Metals for Organic Synthesis* (Wiley-VCH, Weinheim, Germany, **2004**); c) A. de Meijere, F. Diederich, *Metal-Catalyzed Cross-Coupling Reactions, 2nd, Completely Revised and Enlarged Edition* (Wiley-VCH, Weinheim, Germany, **2004**); d) A. de Meijere, S. Braese, M. Oestreich, *Metal-Catalyzed Cross-Coupling Reactions and More* (Wiley-VCH, Weinheim, Germany, **2014**).

[3] a) P. W. N. M. van Leeuwen, *Homogeneous Catalysis: Understanding the Art* (Kluwer Academic Publishers, Dordrecht, The Netherlands, **2004**); b) P. C. J. Kamer, P.W.N.M. van Leeuwen, *Phosphorus(III) Ligands in Homogeneous Catalysis: Design and Synthesis* (Wiley-VCH, Weinheim, Germany, **2012**); c) R. H. Crabtree, *New. J. Chem.* **2011**, *35*, 18-23; d) W. I. Dzik, J. I. van der Vlugt, J. N. H. Reek, B. de Bruin, *Angew. Chem. Int. Ed.* **2011**, *50*, 3356-3358; *Angew. Chem.* **2011**, *123*, 3416-3418; e) H. Grützmacher, *Angew. Chem. Int. Ed.* **2008**, *47*, 1814-1818; *Angew. Chem.* **2008**, *120*, 1838-1842; f) J. I. van der Vlugt, *Eur. J. Inorg. Chem.* **2012**, 363-375; g) J. Meeuwissen, J. N. H. Reek, *Nat. Chem.* **2010**, *3*, 615-621; h) A. J. Sandee, J. N. H. Reek, *Dalton Trans.* **2006**, 3385-3391; i) S. Carboni, C. Gennari, L. Pignataro, U. Piarulli, *Dalton Trans.* **2011**, *40*, 4355-4373.

[4] a) D. Schroeder, S. Shaik, H. Schwarz, *Acc. Chem. Res.* **2000**, *33*, 139-145; b) W. Kaim, *Eur. J. Inorg. Chem.* **2012**, 343-348; c) V. Lyaskovskyy, B. de Bruin, *ACS Catal.* **2012**, *2*, 270-279; d) K. Hindson, B. de Bruin, *Eur. J. Inorg. Chem.* **2012**, 340-342; e) P. J. Chirik, *Inorg. Chem.* **2011**, *50*, 9737-9740; f) O. R. Luca, R. H. Crabtree, *Chem. Soc. Rev.* **2013**, *42*, 1440-1459.

[5] a) S. Kuwata, T. Ikariya, *Chem. Eur. J.* **2011**, *17*, 3542-3556; b) S. Schneider, J. Meiners, B. Askevold, *Eur. J. Inorg. Chem.* **2012**, 412-429; c) B. Zhao, Z. Han, K. Ding, *Angew. Chem. Int. Ed.* **2013**, *52*, 4744-4788; *Angew. Chem.* **2013**, *125*, 4844-4889.

[6] a) C. J. Brown, F. D. Toste, R. G. Bergman, K. N. Raymond, *Chem. Rev.* **2015**, *115*, 3012-3035; b) S. H. A. M. Leenders, R. Gramage-Doria, B. de Bruin, J. N. H. Reek, *Chem. Soc. Rev.* **2015**, *44*, 433-448; f) S. Zarra, D. M. Wood, D. A. Roberts, J. R. Nitschke, *Chem. Soc. Rev.* **2015**, *44*, 419-432; g) L. Catti, Q. Zhang, K. Tiefenbacher, *Synthesis* **2016**, *48*, 313-328.

[7] a) P. W. N. M. van Leeuwen, *Supramolecular Catalysis* (Wiley-VCH, Weinheim, Germany, **2008**); b) M. Raynal, P. Ballester, A. Vidal-Ferran, P. W. N. M. van Leeuwen, *Chem. Soc. Rev.* **2014**, *43*, 1660-1733; c) P. Dydio, J. N. H. Reek, *Chem. Sci.* **2014**, *5*, 2135-2145.

[8] R. H. Crabtree, *Chem. Rev.* **2015**, *115*, 127-150.

[9] a) T. Eicher, S. Hauptmann, A. Speicher, H. Suschitzky, *The Chemistry of Heterocycles: structure, reactions, synthesis and applications* (Wiley-VCH, Weinheim, Germany, **2008**); b) G. Jones, *Comprehensive Heterocyclic Chemistry II, Vol. 5* (Eds. A.R. Katritzky, C.W. Rees, E.F.V Scriven, A. McKillop, Pergamon, Oxford **1996**, pp. 167-243); c) J.A. Joule, K. Mills, *Hetrocyclic Chemistry 4th ed.* (Blackwell Science, Cambridge, **2000**, pp. 63-120).

[10] J. Liu, X. Zhang, H. Yi, C. Liu, R. Liu, H. Zhang, K. Zhuo, A. Lei, *Angew. Chem. Int. Ed.* **2015**, *54*, 1261-1265; *Angew. Chem.* **2015**, *127*, 1277-1281.

[11] a) N. Miyaura, A. Suzuki, *Chem. Rev.* **1995**, *95*, 2457-2483; b) R. Martin, L. Buchwald, *Acc. Chem. Res.* **2008**, *41*, 1461-1473; c) A. F. Littke, G. C. Fu, *Angew. Chem. Int. Ed.* **2002**, *41*, 4176-4211; *Angew. Chem.* **2002**, *114*, 4350-4386.

[12] a) V. Farina, *Adv. Synth. Catal.* **2004**, *346*, 1553-1582; b) N. T. S. Phan, M. Van der Sluys, C. W. Jones, *Adv. Synth. Catal.* **2006**, *348*, 609-679.

[13] a) Y.-G. Zhou, *Acc. Chem. Res.* **2007**, *40*, 1357-1366; b) D.-S. Wang, Q.-A. Chen, S.-M. Lu, Y.-G. Zhou, *Chem. Rev.* **2012**, *112*, 2557-2590; c) F. Glorius, *Org. Biomol. Chem.* **2005**, *3*, 4171-4175; d) R. Kuwano *Heterocycles* **2008**, *76*, 909-922; e) N. Fleury-Brégeot, V. de la Fuente, S. Castillón, C. Claver, *ChemCatChem* **2010**, *2*, 1346-1371; f) H.-U. Blaser, C. Malan, B. Pugin, F. Spindler, H. Steiner, M. Studer, *Adv. Synth. Catal.* **2003**, *345*, 103-151.

[14] a) L.-C. Campeau, S. Rousseaux, K. Fagnou, *J. Am. Chem. Soc.* **2005**, *127*, 18020-18021; b) J.-P. Leclerc, K. Fagnou, *Angew. Chem. Int. Ed.* **2006**, *45*, 7781-7786, *Angew. Chem.* **2006**, *118*, 7945-7950; c) K. S. Kanyiva, Y. Nakao, T. Hiyama, *Angew. Chem. Int. Ed.* **2007**, *46*, 8872-8874, *Angew. Chem.* **2007**, *119*, 9038-9030.

[15] a) K.M. Kadish, K.M. Smith, R. Guilard, *Handbook of Porphyrin Science Vol 1-35*, World Scientific Publishing; b) T. Imamura, K. Fukushima, *Coord. Chem. Rev.* **2000**, *198*, 133-156; c) S. Belanger, M. H. Keefe, J. L. Welch, J. T. Hupp, *Coord. Chem. Rev.* **1999**, *190-192*, 29-45; d) H. E Thoma, K. Araki, *Coord. Chem. Rev.* **2000**, *196*, 307-329; e) J. Wojaczynksi, L. Latos-Grazynski, *Coord. Chem. Rev.* **2000**, *204*, 113-171; f) S. Durot, J. Taesch, V. Heitz, *Chem. Rev.* **2014**, *114*, 8542-8578; g) I. Beletskaya, V. S. Tyurin, A. Y. Tsivadze, R. Guilard, C. Stern, *Chem. Rev.* **2009**, *109*, 1659-1713; h) J. A. A. W. Elemans, V. F. Slagt, A. E. Rowan, R. J. M. Nolte, *Isr. J. Chem.* **2005**, *45*, 271-279; i) A. W. Kleij, J. N. H. Reek, *Chem. Eur. J.* **2006**, *12*, 4218-4227; j) K. S. Suslick, N. A. Rakow, M. E. Kosal, J.-H. Chou, *J. Porphyrins Phtalocyanines* **2000**, *4*, 407-413; k) K. M. Kadish, D. J. Leggett, D. Chang, *Inorg.*

Accepted Manuscript

This article is protected by copyright. All rights reserved.

Chem. **1982**, *21*, 3618-3622; l) M. Hoshino, *Inorg. Chem.* **1986**, *25*, 2476-2478; m) V. F. Slagt, J. N. H. Reek, P. C. J. Kamer, P. W. N. M. van Leeuwen, *Angew. Chem. Int. Ed.* **2001**, *40*, 4271-4274; *Angew. Chem.* **2001**, *113*, 4401-4404; n) A. W. Kleij, M. Lutz, A. L. Speck, P. W. N. M. van Leeuwen, J. N. H. Reek, *Chem. Commun.* **2005**, 3661-3663.

[16] The pyrrolic protons on metalloporphyrins are protected towards reactivity by the *meso*-susbtituents, see: H. Yorimitsu, A. Osuka, *Asian J. Org. Chem.* **2013**, *2*, 356-373.

[17] T. Besset, D. W. Norman, J. N. H. Reek, *Adv. Synth. Catal.* **2013**, *355*, 348-352.

[18] For transmetallation of zinc(II)-porphyrins, see: a) G. Lipiner, I. Willner, Z. Aizenshtat, *J. Chem. Soc., Chem. Commun.* **1985**, 305-306.

[19] For transmetallation of zinc(II)-salphens, see: a) E. C. Escudero-Adán, J. Benet-Buchholz, A. W. Kleij, *Dalton Trans.* **2008**, 734-737; b) E. C. Escudero-Adán, J. Benet-Buchholz, A. W. Kleij, *Inorg. Chem.* **2007**, *46*, 7265-7267.

[20] a) D. J. Darensbourg, J. R. Wildeson, J. C. Yarbrough, *Inorg. Chem.* **2002**, *41*, 973-980; b) V. Zelenak, M. Sabo, W. Massa, P. Llewellyn, *Inorg. Chim. Acta* **2004**, *357*, 2049-2059; c) A. Karmakar, R. J. Sarma, J. B. Baruah, *Inorg. Chem. Commun.* **2006**, *9*, 1169-1172.

[21] For negligible binding ($K_{1:1} < 1$) of *ortho*-substituted pyridines to zinc(II)-porphyrins, see: a) M. Morisue, T. Morita, Y. Kuroda, *Org. Biomol. Chem.* **2010**, *8*, 3457-3463; b) J. S. Summers, A. M. Stolzenberg, *J. Am. Chem. Soc.* **1993**, *115*, 10559-10567; c) C. H. Kirksey, P. Hambright, C. B. Storm, *Inorg. Chem.* **1969**, *8*, 2141-2144; d) R. J. Abraham, G. R. Bedford, B. Wright, *Org. Magn. Reson.***1982**, *18*, 45-52; e) G. Szintay, A. Horváth, *Inorg. Chim. Acta* **2000**, *310*, 175-182.

[22] a) P. Thordarson, *Chem. Soc. Rev.* **2011**, *40*, 1305-1323; b) P. Dydio, T. Zielinski, J. Zurczak, *J. Org. Chem.* **2009**, *74*, 1525-1530; c) F. Ulatowski, K. Dabrowa, T. Balakier, J. Jurczak, *J. Org. Chem.* **2016**, *81*, 1746-1756. For examples of small UV-vis changes upon pyridine titration, see: d) V. Bocokic, M. Lutz, A. L. Spek, J. N. H. Reek, *Dalton Trans.* **2012**, *41*, 3740-3750; e) D. Anselmo, V. Bocokic, A. Decortes, E. C. Escudero-Adán, J. Benet-Buchholz, J. N. H. Reek, A. W. Kleij, *Polyhedron*, **2012**, *32*, 49-53.

[23] K. M. Kadish, L. R. Shiue, R. K. Rhodes, L. A. Bottomley, *Inorg. Chem.* **1981**, *20*, 1274-1277.

[24] S. K. Samanta, D. Samanta, J. W. Bats, M. Schmittel, *J. Org. Chem.* **2011**, *76*, 7466-7473.

[25] a) A. De Santis, A. Forni, R. Liantonio, P. Metrangolo, T. Pilati, G. Resnati, *Chem. Eur. J.* **2003**, *9*, 3974-3983; b) Q. Chu, Z. Wang, Q. Huang, C. Yan, S. Zhu, *New. J. Chem.* **2003**, *27*, 1522-1527; c) R. W. Troff, T. Mäkelä, F. Topić, A. Valkonen, K. Raatikainen, K. Rissanen, *Eur. J. Org. Chem.* **2013**, 1617-1637; d) P. Metrangolo, F. Meyer, T. Pilati, G. Resnati, G. Terraneo, *Angew. Chem. Int. Ed.* **2008**, *47*, 6114-6127; *Angew. Chem.* **2008**, *120*, 6206-6220.

[26] For zinc(II)-salphens binding to *ortho*-substituted pyridines, see: a) E. C. Escudero-Adán, J. Benet-Buchholz, A. W. Kleij, *Eur. J. Inorg. Chem.* **2009**, 3562-3568.

[27] For similar non-optimal coordination between phosphanes and metal cations see: a) R. Gramage-Doria, D. Armspach, D. Matt, L. Toupet, *Angew. Chem. Int. Ed.* **2011**, *50*, 1554-1559; *Angew. Chem.* **2011**, *123*, 1592-1597; b) R. Gramage-Doria, D. Armspach, D. Matt, L. Toupet, *Dalton Trans.* **2012**, *41*, 8786-8796.

[28] a) M. Nishio, M. Hirota, Y. Umezawa, *The CH/π Interaction. Evidence, Nature, and Consequences*, Wiley-VCH, New York, **1998**; b) G. R. Desiraju, T. Steiner, *The Weak Hydrogen Bonds in Chemistry and Structural Biology*, Oxford University Press, Oxford, **1999**; c) M. Nishio, *Weak Hydrogen Bonds* in *Encyclopedia of Supramolecular Chemistry* (Eds.: J. L. Atwood, J. W. Steed), Marcel Dekker Inc., New York, **2004**, 1576-1585.

[29] a) O. Hassel, K. O. Strømme, *Acta Chem. Scand.* **1958**, *12*, 1146-1147; b) A. V. Vasilyev, S. V. Lindeman, J. K. Kochi, *Chem. Commun.* **2001**, 909-910; c) D. Lenoir, *Angew. Chem. Int. Ed.* **2003**, *42*, 854-857; *Angew. Chem.* **2003**, *115*, 880-883; d) G. Cavallo, P. Metrangolo, R. Milani, T. Pilati, A. Priimagi, G. Resnati, G. Terraneo, *Chem. Rev.* **2016**, *116*, 2478-2601.

[30] a) C. A. Hunter, J. K. M. Sanders, *J. Am. Chem. Soc.* **1990**, *112*, 5525-5534; b) G. R. Desiraju, A. Gavezzotti, *J. Chem. Soc. Chem. Commun.* **1989**, 621-623; c) S. Tsuzuki, K. Honda, T. Uchimaru, M. Mikami, K. Tanabe, *J. Am. Chem. Soc.* **2002**, *124*, 104-112.

[31] F. Bellina, A. Carpita, R. Rossi, *Synthesis* **2004**, *15*, 2419-2440; b) A. Suzuki, *Angew. Chem. Int. Ed.* **2011**, *50*, 6722-6737; *Angew. Chem.* **2011**, *123*, 6854-6869; c) F. Alonso, I. P. Beletskaya, M. Yus, *Tetrahedron* **2008**, *64*, 3047-3101.

[32] a) J. R. Miller, G. D. Dorough, *J. Am. Chem. Soc.* **1952**, *74*, 3977-3981; b) G. C. Vogel, L. A. Searby, *Inorg. Chem.* **1973**, *12*, 936-939; c) G. C. Vogel, B. A. Beckman, *Inorg. Chem.* **1976**, *15*, 483-484.

[33] For $^{31}P\{^{1}H\}$ NMR spectra of similar palladium-phosphane complexes, see: a) C. Amatore, E. Carré, A. Jutand, M. A. M'Barki, G. Meyer, *Organometallics* **1995**, *14*, 5605-5614; b) A. Jutand, S. Négri, J. G. de Vries, *Eur. J. Inorg. Chem.* **2002**, 1711-1717; c) M. Irandoust, M. Joshaghani, E. Rafiee, M. Pourshahbaz *Spec. Acta Part A* **2009**, *74*, 855-859.

[34] For hydroxyl-mediated cleavage of imine bonds belonging to zinc(II)-salphen building blocks, see: E. C. Escudero-Adán, M. Martínez Belmonte, J. Benet-Buchholz, A. W. Kleij, *Org. Lett.* **2010**, *12*, 4592-4595.

[35] a) S. Brase, A. de Meijere, *Metal-Catalyzed Cross-Coupling Reactions, 2nd, Completely Revised and Enlarged Edition* (Wiley-VCH, Weinheim, Germany, **2004**), pp 217-315; b) I. P. Beletskaya, A. V. Cheprakov, *Chem. Rev.* **2000**, *100*, 3009-3066; c) W. Cabri, I. Candiani, *Acc. Chem Res.* **1995**, *28*, 2-7.

[36] a) V. S. Thirunavukkarasu, S. I. Kozhushkov, L. Ackermann, *Chem. Commun.* **2014**, *50*, 29-39; b) L. Ackermann, *Acc. Chem. Res.* **2014**, *47* 281-295; c) P. B. Arockiam, C. Bruneau, P. H. Dixneuf, *Chem. Rev.* **2012**, *112*, 5879-5918.

[37] a) L. Ackermann, R. Vicente, A. Althammer, *Org. Lett.* **2008**, *10*, 2299-2302; b) F. Pozgan, P. H. Dixneuf, *Adv. Synth. Catal.* **2009**, *351*, 1737-1743.

[38] A. M. Lifschitz, M. S. Rosen, C. M. McGuirk, C. A. Mirkin, *J. Am. Chem. Soc.* **2015**, *137*, 7252-7261.

[39] a) V. Blanco, D. A. Leigh, V. Marcos, *Chem. Soc. Rev.* **2015**, *44*, 5341-5370; b) U. Lüning, *Angew. Chem. Int. Ed.* **2012**, *51*, 8163-8165; *Angew. Chem.* **2012**, *124*, 8285-8287.

[40] a) A. D. Adler, F. R. Longo, J. D. Finarelli, J. Goldmacher, J. Assour, L. Korsakoff, *J. Org. Chem.* **1967**, *32*, 476; b) J. B. Cooper, C. T. Brewer, *Inorg. Chim. Acta* **1987**, *129*, 25-30.

[41] M. Kuil, P. E. Goudriaan, P .W. N. M. van Leeuwen, J. N. H. Reek, *Chem. Commun.* **2006**, 4679-4681.

[42] a) E. Busto V. Gotor-Fernández, V. Gotor, *Adv. Synth. Catal.* **2006**, *348*, 2626-2632; b) M. Mallet, G. Quéguiner, *Tetrahedron* **1982**, *38*, 3035-3042.

[43] www.supramolecular.org

Accepted Manuscript

This article is protected by copyright. All rights reserved.

10.1002/chem.201604780

WILEY-VCH

Entry for the Table of Contents

FULL PAPER

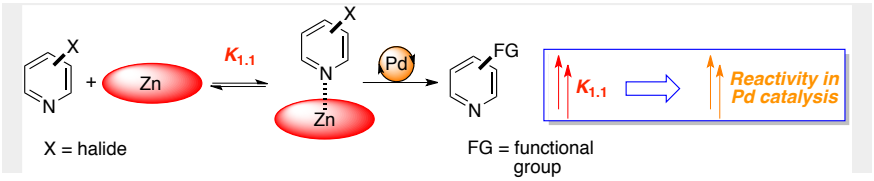

*M. Kadri, J. Hou, V. Dorcet, T. Roisnel, L. Bechki, A. Miloudi, C. Bruneau, and R. Gramage-Doria**

Page No. – Page No.

Palladium-catalyzed cross-coupling reactions controlled by non-covalent Zn···N interactions

Useful weakness: The reactivity of halopyridine substrates in palladium-catalyzed cross-coupling reactions has been controlled via weak, non-covalent interactions between substrates and catalytically inert zinc(II)-containing porphyrins and salphens. The binding strength between the substrates and the zinc(II)-containing scaffolds prevents undesired halopyridine···palladium over-coordination (catalyst inhibition), which indirectly leads to an increase of the efficiency of the catalyst.

WILEY-VCH
Accepted Manuscript

This article is protected by copyright. All rights reserved.